NJC

PAPER

View Article Online
View Journal | View Issue

Cite this: *New J. Chem.*, 2014, **38**, 2016

Microwave-assisted post-synthesis modification of layered simple hydroxides†

O. Palamarciuc,[abc] E. Delahaye,[ab] P. Rabu[ab] and G. Rogez*[ab]

Received (in Montpellier, France) 7th October 2013,
Accepted 20th November 2013

DOI: 10.1039/c3nj01231j

www.rsc.org/njc

A new method to functionalize layered simple hydroxides by post-synthesis modification is described. A layered cobalt hydroxide was modified with a molecule bearing a free amino group. We show here that it is possible to post-functionalize the metal hydroxide layers by performing *in situ* microwave assisted reactions with the free amino group, constituting a new appealing strategy for functionalization of layered solids. The obtained compounds are characterized by ancillary techniques and their magnetic properties were investigated, which show that the inorganic magnetic layers are not deeply affected by the post-functionalization process.

Introduction

Since the discovery of the outstanding electronic properties of the graphene derivatives,[1] the research into functional nanomaterials has been increasingly concerned with the conception of new multifunctional nanosheet-based systems,[2,3] with intensification of research in the field of layered materials.[4,5] Among the possible chemical routes, the hybrid organic–inorganic approach is particularly well suited to promote multifunctionality within a single material. It is indeed possible to control the assembly at the nanoscale level of two components, each bearing its own properties.[6–8] In that way, each sub-network exhibits its own properties or contributes synergistically to new physical phenomena and novel applications.[9,10]

Transition metal layered simple hydroxides (LSH), of general formula $M^{II}_2(OH)_3(X)\cdot mH_2O$ (M = Co, Cu, Ni and X is an easily substitutable anion, nitrate or acetate for instance), are very well adapted to grafting reactions of various organic molecules. We and others have recently obtained hybrid compounds based on LSH functionalized with (oligo)thiophenes,[11,12] azo dyes,[13] diarylethene,[14] or complexes of transition metals.[15–19] We have notably developed a pre-intercalation procedure which enables the insertion–grafting of large molecules due to the preswelling of the layered host.[13] However, a major drawback of the functionalization reactions of layered hydroxides lies in the fact that they proceed by anion-exchange reaction, especially effective in aqueous medium at basic pH (typically around pH = 8). The pre-intercalation strategy allows for partial stabilization of species sensitive to hydrolysis, by creating a hydrophobic environment in-between the inorganic layers.[15] But the ion-exchange reaction still requires the use of water, even when pre-intercalation is used. This severely limits the type of molecules that can be considered to be grafted in the interlamellar space. To overcome this difficulty, one solution is to synthesize *in situ* (in the interlamellar space) the desired molecules from a pre-grafted functional precursor. Thus, only the first stage (grafting the precursor) requires the use of insertion-grafting conditions by anion exchange. The following reactions may appeal to a much larger panel of conditions, including the use of non-aqueous solvents. Confinement of the reaction space may also have specific effects on the synthesis.

The post-synthesis modification strategy has been widely developed for Metal Organic Frameworks[20–27] or for mesoporous silicates.[28,29] Yet, to our knowledge it has seldom been used in layered materials. One noticeable example concerns the controlled 2D growth of Prussian blue analogues in the interlamellar space of Layered Double Hydroxides (LDH).[30,31] In this example, a Prussian blue analogue is synthesized in a two-step reaction. Hexacyanometalate is first inserted in the interlamellar space of LDH, then a M(II) salt is reacted with the hybrid, and the *in situ* reaction leads to the formation of a Prussian blue analogue in-between the inorganic layers. Another example deals with confined synthesis of pyridinic and pyrrolic nitrogen-doped graphene in layered montmorillonite.[32] Yet, *stricto-sensu*, these examples are not really representative of a post-synthesis modification. According to Cohen,[22] post-synthesis modification can be broadly defined as "a chemical derivatization of MOFs after their formation"; in a more strict sense, it may refer only to those modifications involving covalent bonds[22] or dative bonds[25]

[a] *Institut de Physique et Chimie des Matériaux de Strasbourg, UMR 7504 CNRS - Université de Strasbourg, and Labex NIE, 23 rue du Loess, BP 43, 67034 Strasbourg cedex 2, France. E-mail: rogez@unistra.fr*
[b] *Fondation icFRC International Center for Frontier Research in Chemistry, 8, allée Gaspard Monge, F-67000 Strasbourg, France*
[c] *State University of Moldova, Mateevici 60, Chisinau MD-2009, Republic of Moldova*

† Electronic supplementary information (ESI) available: SEM images of all compounds. See DOI: 10.1039/c3nj01231j

with the framework or deprotection.[25] (In the present proposed extension of definition "MOFs" may be replaced by "hybrid solids".)

We report in this article the post-synthesis modification of a Co LSH, functionalized with *p*-amino-benzoic acid. We show that the amine groups react *in situ* with various aldehydes (aliphatic and aromatic) to form imines (azomethine groups). Interestingly, conventional activation (heating) is inefficient in the present case, whereas microwave irradiation enables the *in situ* reaction. This technique constitutes a new appealing strategy for functionalization of layered structures.

Results and discussion

We investigated the functionalization of layered cobalt hydroxide acetate, $\mathbf{Co_2(OH)_3(OAc)\cdot H_2O}$, the structure of which is presented in Fig. 1.

The general strategy we have followed is schematized in Scheme 1. We have chosen the *in situ* formation of various alkyl or aryl imino-benzoates as a model reaction to validate the concept of post-functionalization in layered metal hydroxides.

In the first step, a layered Co hydroxide was functionalized with *p*-amino-benzoic acid providing (4-NH_2–BzAc)⊂Co (**1**) by classical anion exchange. The initial pH has to be carefully set at 8 ± 0.2. Larger values lead to low crystallinity and to Co-oxide impurities, whereas lower values lead to a mixture of unidentified non-lamellar phases. The use of ethanol along with water (ethanol–water = 1/4 (v:v)) is also crucial, as ethanol may serve as an antioxidant.

The second step deals with the post-functionalization itself. Compound **1** is made to react with aldehydes, which likely condense with the free amino groups to give imines, sketched in Scheme 1, and water. Yet, all attempts to perform this reaction using classical heating (up to 80 °C), in dry solvents (alcohols, toluene, and chloroform) led to the recovery of the starting material. In order to overcome this difficulty, the reactions were then performed using microwave activation under autogeneous pressure. The best conditions were found to be: absolute

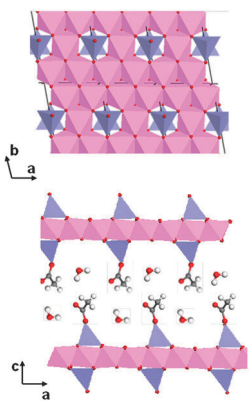

Fig. 1 Structure of $\mathbf{Co_2(OH)_3(OAc)\cdot H_2O}$ ($R\bar{3}m$, a = 0.313 nm, c = 1.27 nm, α-$Co(OH)_2$ polytype).[33–36] Pink and purple polyhedra hold for Co(II) ions in octahedral and tetrahedral sites respectively.

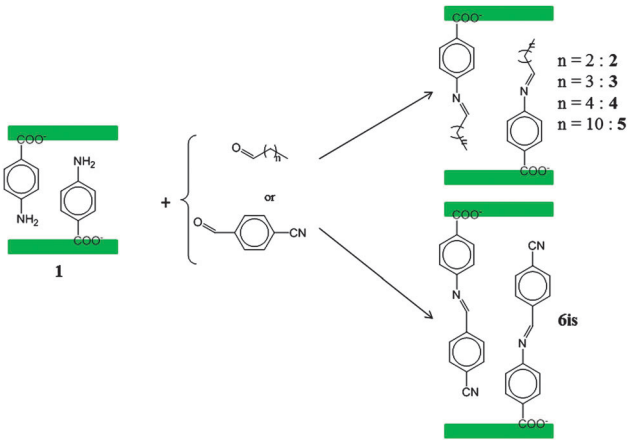

Scheme 1 Post-synthesis modification strategy.

ethanol as solvent (20 mL in a sealed microwave tube of 30 mL), 0.5 moles of **1**, 3 equivalents of aldehyde and 30 W microwave irradiation for 10 min. Under these conditions the pressure in the microwave tube reached typically 9 bar and the temperature increased up to 140 °C. Microwave activation has proved to be particularly useful to accelerate reactions, to increase the yields and the purity of compounds under milder reaction conditions and to obtain products which cannot be obtained otherwise. It has essentially been used in organic chemistry,[37] but also in coordination chemistry[38–40] and in materials chemistry.[41,42] It has also been used for the post-functionalization of nanoparticles[43] or of MOFs,[25,44–47] but to the best of our knowledge it is the first time microwave heating is used for the internal post-synthesis modification of layered hybrid solids which are stable in a reduced range of pH.

It is worth noting here that it has not been necessary to preliminarily dehydrate the starting compound (4-NH_2–BzAc)⊂Co (**1**) even though it contains 2.4 water molecules per formula unit. It was neither necessary to remove water which forms during the reaction, contrary to what is usually done to displace the equilibrium of reactions which produce water as a by-product (using molecular sieves for instance, or Dean–Stark apparatus). The water molecules which form remain within the product, as attested by elemental analysis, and are probably engaged in H-bonding with the inorganic hydroxy network.

Two kinds of aldehyde have been chosen to react with the amino group of the pre-grafted amino-benzoate: aliphatic aldehydes, with various alkyl chain lengths (butanal, pentanal, hexanal and dodecanal) and one aromatic aldehyde (4-cyanobenzaldehyde), bearing a cyano group to serve as an IR marker.

In addition, the imine **LH** formed from the condensation of 4-aminobenzoic acid with 4-cyanobenzaldehyde was isolated and further grafted into the interlamellar space of $\mathbf{Co_2(OH)_3(OAc)\cdot H_2O}$ by "classical" ion exchange. This compound, denoted **6ae**, served for comparison with the compound obtained by *in situ* reaction, denoted **6is**. Notably, it has not been possible to insert the other preformed imine ligands by ion-exchange. The yields of the post-synthesis modification reactions are all around 80%. The yield of **6ae** is notably lower, around 60%. This underlines

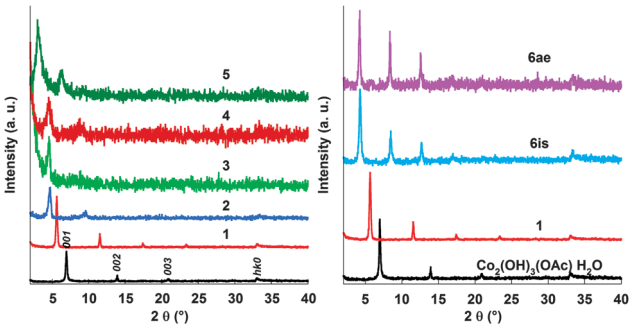

Fig. 2 Powder X-ray diffraction patterns for compounds **1–5**, **6is**, **6ae** and the starting compound **$Co_2(OH)_3(OAc)\cdot H_2O$** (black).

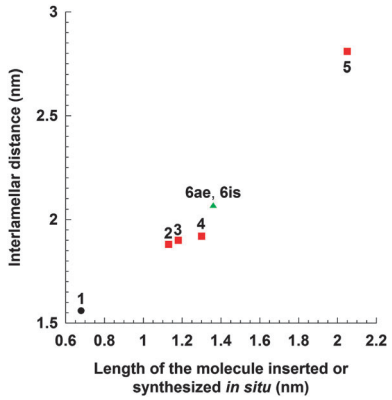

Fig. 3 Correlation between the interlamellar distance of the hybrid compounds and the size of the molecule inserted or synthesized *in situ*. Color stands for the family of compounds (black for the starting compound **1**, red for the compounds with aliphatic chains **2–5**, and green for the compounds with the cyanobenzyl group **6is** and **6ae**).

the relative efficiency of the microwave assisted post-synthetic modification with respect to functionalization by ion exchange.

Interestingly, despite the reversible character of the imine formation reaction, it has not been possible to hydrolyze the imine formed within the interlamellar space (while keeping the integrity of the inorganic host), regardless of the activation used (classical or microwave).

The products were first characterized by powder X-ray diffraction (Fig. 2).

The XRD pattern of all compounds shows intense 00*l* diffraction peaks at low angle which evidences their lamellar structure. For **1**, **6ae** and **6is**, up to four harmonics are visible, whereas for compounds **2–5**, only two harmonics are visible, which underlines their lower crystallinity. In the high angle region, all XRD patterns exhibit similar asymmetrical peaks at $2\theta = 33^\circ$ (Cu Kα_1 = 0.1540598 nm) corresponding to in-plane diffraction lines. The asymmetry suggests turbostratic disorder. The interlamellar distances for all compounds are collected in Table 1.

The important feature is that the interlamellar distance increases gradually when the size of the aldehyde increases. For small alkyl chains (compounds **2**, **3** and **4**), the variation of the interlamellar spacing is linear with the number of carbon atoms of the alkyl chain. For the long alkyl chain (compound **5**) a discontinuity occurs (with respect to the other aliphatic compounds) which is likely due to a change in the interdigitation of the molecules. Fig. 3 shows a clear correlation between the size of the molecule[48] which is supposed to form in the interlamellar space and the interlamellar distance of the hybrid compounds, which constitute further evidence for the *in situ* reaction.

The XRD patterns of **6is** and **6ae** are similar, but the XRD pattern of **6ae** reveals slightly broader peaks, especially at 33°, suggesting a lower crystallinity. Thus *in situ* post-synthesis modification leads to the same material as direct ion exchange.

Table 1 Interlamellar spacing of the hybrid compounds **1–5**, **6is** and **6ae**

Compound	Inserted molecule	Interlamellar distance (nm)
$Co_2(OH)_3(OAc)\cdot H_2O$	OAc	1.27
1	4-NH_2–BzAc	1.56
2	AcBz–N=CH–C_3H_7	1.88
3	AcBz–N=CH–C_4H_9	1.90
4	AcBz–N=CH–C_5H_{11}	1.92
5	AcBz–N=CH–$C_{11}H_{23}$	2.81
6is	AcBz–N=CH–Bz–CN	2.07
6ae	AcBz–N=CH–Bz–CN	2.07

Even though it is not possible to claim from elemental analysis that only the *in situ* formation of imine took place, the results of the elemental analysis confirm the presence of additional organic moieties with respect to the starting compound **1**. The post-synthesis modification procedure induces a small loss of the grafted ligand: with respect to the general formula $Co_2(OH)_{4-x}(L)_x$, x = 0.65 for **1**, whereas x is slightly smaller for **2–5** and for **6is**, ranging from 0.43 to 0.53. For **6ae** x is of the same order of magnitude as for **1** (x = 0.62). This observation underlines that despite post-synthesis modification is supposed to let the inorganic matrix untouched, the mechanism is most probably more complicated. The inorganic network probably readjusts its structure to adapt the layers to the new molecular area of the organic components. In the case of compounds obtained by *in situ* reaction, this rearrangement leads to partial leaching of amino-benzoate molecules. Therefore, compounds **6ae** and **6is**, although of similar structure, are slightly different in composition.

Unfortunately, the attempts to characterize the functionalization of the samples by means of solid state ^{13}C NMR spectroscopy were unsuccessful. This is likely due to a broadening of the signal caused by the slowly relaxing paramagnetic Co^{II} ions. Nevertheless, the compounds were further characterized by infrared spectroscopy (Fig. 4). Principal characteristic bands are collected in Table 2.

The first noticeable feature is that in all hybrid compounds **1–5**, **6is** and **6ae**, the position of the carboxylate vibration bands hardly changes. The asymmetric band corresponding to the asymmetric vibration mode is around 1540 cm^{-1} whereas the one corresponding to the symmetric vibration mode is around 1390 cm^{-1}. For comparison, these bands are located at 1682 cm^{-1} and 1429 cm^{-1}, respectively, for the free ligand **LH**. The position of the bands as well as the value of $\Delta\nu = \nu_{as} - \nu_s$ indicates that the carboxylate is coordinated to the inorganic layers, in a unidentate mode.[49–52]

In **1**, the bending vibration of the free amine groups is visible at 1610 cm^{-1} whereas their stretching vibration at

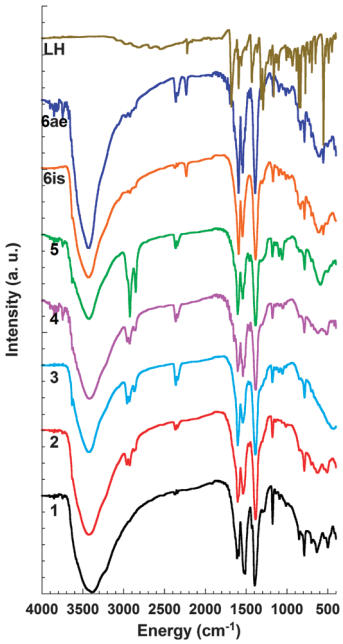

Fig. 4 FTIR spectra of compounds **1–5**, **6is**, **6ae** and of the imine **LH**.

higher energy is masked by the stretching vibration of the water molecules.

The similarity between the spectra of **6is** and **6ae** confirms that the two compounds are indeed identical as evidenced from elemental analysis and X-ray diffraction.

Several features confirm that additional organic moieties are present in the hybrid compounds. The CH_2 and CH_3 vibrations are clearly identified in the 2850–3000 cm^{-1} region for compounds **2–5**. In addition, the intensity of these bands increases with the length of the alkyl chain of the aldehyde used. For **6ae** and **6is**, the cyanide vibration band is clearly visible at 2235 cm^{-1} indicating the presence of the cyanobenzene moiety.

Finally indications concerning the effectiveness of the *in situ* formation of the imine functions in the hybrid compounds **2–5** and **6is** are given by the disappearance of the NH_2 bending vibration at 1610 cm^{-1}, the absence of the characteristic vibration of the aldehyde group at 1700 cm^{-1} and the appearance in all compounds of the imine vibration band around 1600 cm^{-1}.

The SEM images of compounds **1** and **4** are shown in Fig. 5 and are representative of all hybrid compounds reported here (see Fig. S1, ESI†). They are obtained as thin platelets, in agreement

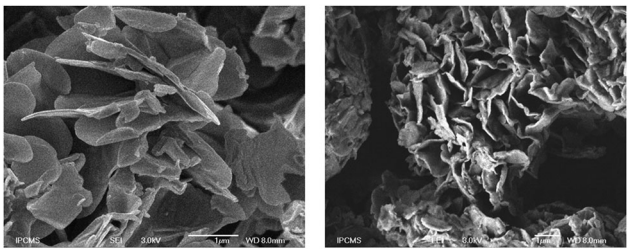

Fig. 5 SEM images of compounds **1** (left) and **4** (right).

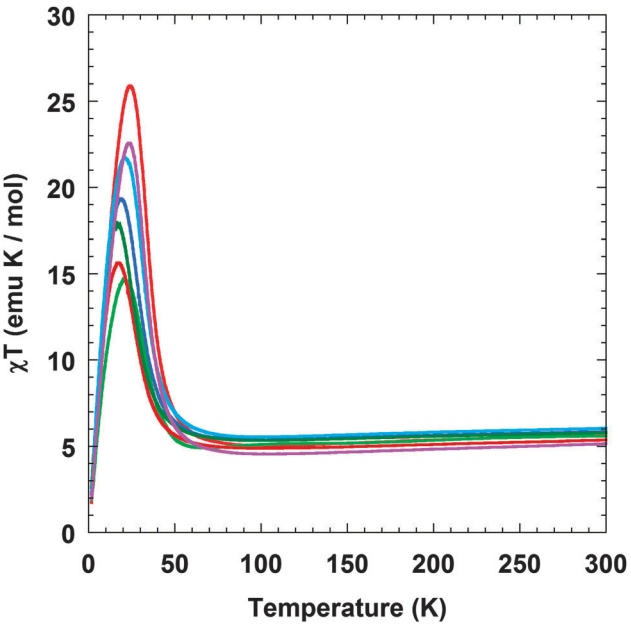

Fig. 6 $\chi T = f(T)$ under 0.5 T for compounds **1** (red), **2** (dark blue), **3** (light green), **4** (brown), **5** (dark green), **6is** (light blue) and **6ae** (purple).

with the lamellar character of their structure. No particular difference in shape, size or morphology was noticed whether the compounds were obtained by post-synthesis modification or by anion exchange.

The magnetic behaviors of all compounds are much alike (Fig. 6). The Curie constants, determined from the fit of $1/\chi = f(T)$ to the Curie–Weiss law, are all within the range 5.69–6.27 emu K mol^{-1}, in agreement with the presence of a mixture of tetrahedral and octahedral high-spin Co(II) ions.[53] Upon cooling, the χT products of all compounds decrease slowly down to a minimum

Table 2 Characteristic infrared absorption bands

Compound	ν(C≡N) (cm^{-1})	$\delta(NH_2)$ (cm^{-1})	ν(C=N) (cm^{-1})	ν_{as}(OAc) (cm^{-1})	ν_s(OAc) (cm^{-1})	$\Delta\nu$ (cm^{-1})
$Co_2(OH)_3(OAc)\cdot H_2O$	/	/	/	1568	1403	165
1	/	1610	/	1528	1393	135
2	/	/	1606	1539	1386	153
3	/	/	1603	1541	1387	154
4	/	/	1605	1539	1385	154
5	/	/	1603	1543	1386	157
6is	2235	/	1593	1546	1385	161
6ae	2235	/	1594	1543	1391	152
LH	2222	/	1592	1682	1429	253

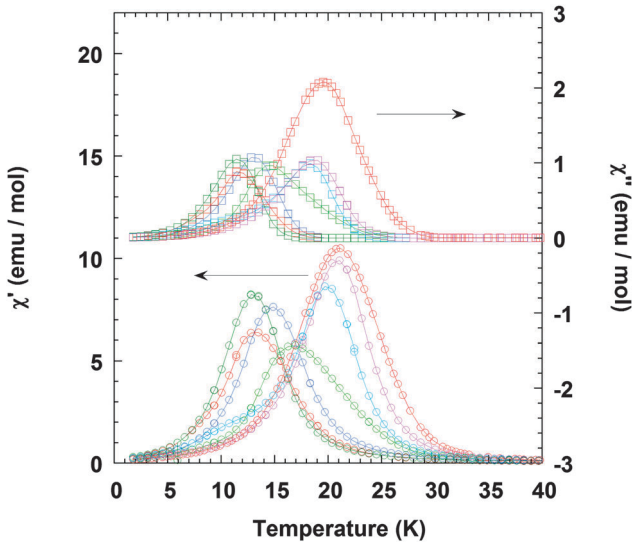

Fig. 7 In-phase susceptibility (χ', bottom, open circles) and out-of-phase susceptibility (χ'', top, open squares) for compounds **1** (red), **2** (dark blue), **3** (light green), **4** (brown), **5** (dark green), **6is** (light blue) and **6ae** (purple) (full lines are just guides for the eye).

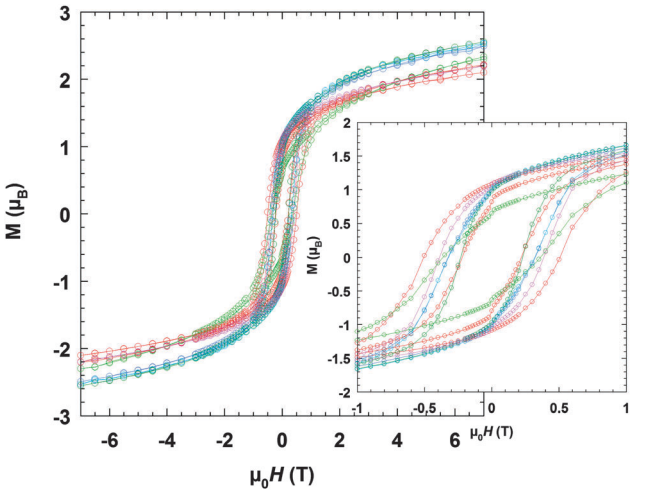

Fig. 8 $M = f(H)$ at 1.8 K for compounds **1** (red), **2** (dark blue), **3** (light green), **4** (brown), **5** (dark green), **6is** (light blue) and **6ae** (purple) (full lines are just guides for the eye). Inset: zoom of the −1/+1 T region.

around 100 K. This behaviour is attributed to spin–orbit coupling for high-spin Co(II) ions in octahedral sites, and/or to antiferromagnetic interactions between the spin carriers. Below this minimum, the χT products diverge, up to a field dependent maximum (around 20 K here under 0.5 T), which is due to the saturation effect.

This peculiar behaviour is attributed to the occurrence of a long range ferromagnetic-type ordering. The ordering temperatures are further determined from the maximum of the in-phase susceptibility, around 15 K for compounds **2–5**, and around 20 K for compounds **1**, **6is** and **6ae** (Fig. 7, and Table 3).

The ferromagnetic-type behaviour is confirmed by the occurrence of out of phase signals. Accordingly, the low temperature magnetization *vs.* field curves (Fig. 8) show the presence of hysteresis loops, with coercive fields around 0.25 T (Table 3). The low value of the moments at high fields, much lower than expected for the total alignment of the moments (4–6 μ_B for two Co(II) ions), supports a ferrimagnetic ordering.[18,53]

The resemblance between the magnetic behaviours of all compounds underlines that the post-synthesis modification does not deeply alter the magnetic properties of the parent compound **1**. Yet two tendencies can be distinguished. The ordering temperatures of compounds **1**, **6is** and **6ae** (21.0 K, 19.8 K and 21.0 K respectively) are indeed significantly larger than the ones of compounds **2–5** (14.9 K, 16.7 K, 13.2 K and 13.0 K respectively). This feature is reminiscent of what has been described in the case of layered Ni(II) organophosphonates.[54] In this family, the magnetic behaviour of the compounds functionalized with long alkyl chain organophosphonates is much different than that of compounds functionalized with short alkyl chain organophosphonates, or with aromatic organophosphonates. This has been ascribed to the chemical pressure induced by the long alkyl chains onto the magnetic layers.[54–56] The resulting distorsions may cause some changes in the in-plane superexchange pathways and in the size of the 2D correlation domains.[57] Moreover, different magnetic dimensionalities (2D to 3D) were pointed out, highlighting the possible role of interlamellar π–π interactions in the interlayer coupling. In the present series of compounds, π-stacking interactions (in the case of **1**, **6is**, and **6ae**) or H-bonding interactions (in the case of **1**) may be responsible for the slightly different coupling mechanism between the layers and hence of different ordering temperature.

Table 3 Magnetic characteristics of compounds **1–5**, **6is** and **6ae**

	C (emu K mol^{-1})	T_N (K)	$\mu_0 H_c$ (T)	$M_{(7\ T)}$ (μ_B)
1	6.29	21.0	0.50	2.1
2	6.27	14.9	0.32	2.5
3	6.11	16.7	0.36	2.3
4	5.87	13.2	0.22	2.2
5	6.20	13.0	0.23	2.6
6is	6.45	19.8	0.33	2.5
6ae	5.69	21.0	0.39	2.2

Conclusions

We have shown here that in addition to classical ion-exchange reactions, the functionalization of layered simple hydroxides can also proceed *via* post-synthesis modification. Post-synthesis modification allows functionalizing LSH in non-aqueous solvent, which is a major advantage. Indeed, LSH may be unstable in water at too low or too high pH. Moreover, the molecules to functionalize the LSH with may be unstable under the conditions of classical ion-exchange. Therefore synthesizing them *in situ* is an interesting strategy to overcome this difficulty.

In this paper we validate the feasibility of such procedure in the case of layered simple hydroxides. We underline the advantage of microwave activation, since classical thermal activation is inefficient in the present case. To the best of our knowledge, it is the first time microwave activation is used to perform post-synthesis

modification of layered solids. We are currently working to extend this strategy to the *in situ* synthesis of other molecules, in order to bring new properties to layered magnetic materials, such as luminescence for instance. This strategy may further be applied to the functionalization of other kinds of layered materials (clays, LDH, layered oxalates, *etc.*). It thus opens up very promising perspectives for the introduction of new functionalities in layered materials, unattainable with the classical functionalization processes.

Experimental

Chemicals were of reagent grade (Alfa-Aesar and Aldrich (cobalt acetate)) and were used without further purification. Microwave syntheses were performed using a microwave synthesis reactor Monowave 300 (Anton Paar). Elemental analyses for C, H, N, and Co were carried out at the Service Central d'Analyse of the CNRS (USR-59). The powder XRD patterns were collected using a Bruker D8 diffractometer (Cu $K\alpha_1$ = 0.1540598 nm) equipped with a SolX detector with energy discrimination. The SEM images were obtained using a JEOL 6700F (scanning electron microscope (SEM) equipped with a field emission gun, operating at 3 kV in the SEI mode). FT-IR spectra were collected on a Digilab FTS 3000 computer-driven instrument (0.1 mm thick powder samples in KBr). Solution ^{1}H NMR spectra were recorded using a Bruker AVANCE 300 (300 MHz) spectrometer. The internal references of the spectrum correspond to the peak of the non-deuterated solvent. The magnetic studies were carried out using a SQUID magnetometer (Quantum Design Squid-VSM) covering the temperature and field ranges 2–300 K, ±7 T. ac susceptibility measurements were performed in a 0.20 mT alternative field (95 Hz). Magnetization measurements at different fields at room temperature confirm the absence of ferromagnetic impurities.

$Co_2(OH)_3(OAc)\cdot H_2O$ was prepared as previously described.[14,58,59]

LH

The imine ligand was synthesized by mixing 4-aminobenzoic acid (1.37 g, 10 mmol) and 4-cyanobenzaldehyde (1.31 g, 10 mmol) in 60 mL of absolute ethanol. After refluxing for 2 h, the reaction was cooled to 5 °C using an ice bath. The light yellow compound was collected by filtration, washed with cold absolute ethanol and dried under vacuum. Yield: 65%.

^{1}H NMR (300 MHz, [D_6]DMSO): δ = 12.92 (1H, s), 8.73 (1H, s), 8.10 (2H, d, J = 8.3 Hz), 7.99 (4H, d, J = 8.3 Hz), 7.35 (2H, d, J = 8.3 Hz) ppm.

(4-NH_2–BzAc)⊂Co (1)

4-Aminobenzoic acid (4-NH_2–BzAc) (822 mg, 6 mmol) was dissolved in water (160 mL) and the pH was adjusted to 8 using NaOH (0.2 mol L^{-1}). At this stage, **$Co_2(OH)_3(OAc)\cdot H_2O$** (496 mg, 2 mmol) was added along with 40 mL of ethanol. The mixture was stirred under argon at room temperature for 48 h. The dark green powder was collected by filtration, washed with water and ethanol, and dried under vacuum. Yield: 85%.

Anal. for $Co_2(OH)_{3.35}$(4-NH_2–BzAc)$_{0.65}\cdot$2.4 H_2O: $Co_2C_{4.55}H_{7.25}N_{0.65}O_{4.65}\cdot$2.4 H_2O (M = 306.55 g mol^{-1}) found (%): Co, 37.92; C, 17.47; H, 3.29; N, 2.62; calcd: Co, 38.45; C, 17.83; H, 3.96; N, 2.97. IR (KBr pellet, cm^{-1}): 3385 (s), 1610 (s), 1528 (s), 1512 (s), 1393 (s), 1177 (m) 852 (w), 789 (m), 635 (w), 501 (w).

(AcBz–N=CH–C_3H_7)⊂Co (2)

1 (153 mg, 0.5 mmol), butyraldehyde (butanal) (108 mg, 1.5 mmol) and 20 mL of absolute ethanol were introduced in a 30 mL sealed microwave vessel. The mixture was placed under the microwave irradiation (30 W) for 10 min. The dark green powder was collected by filtration, washed with ethanol and dried under vacuum. Yield: 80%.

Anal. for $Co_2(OH)_{3.47}$(AcBz–N=CH–C_3H_7)$_{0.53}\cdot$2.8 H_2O: $Co_2C_{5.83}H_{9.83}N_{0.53}O_{4.53}\cdot$2.8 H_2O (M = 328.13 g mol^{-1}) found (%): Co, 35.99; C, 21.26; H, 3.73; N, 2.04; calcd: Co, 35.92; C, 21.34; H, 4.73; N, 2.26. IR (KBr pellet, cm^{-1}): 3426 (s), 2962 (m), 2928 (m), 2873 (w), 1606 (s), 1539 (s), 1386 (s), 1178 (m) 849 (w), 788 (m), 622 (w), 509 (w).

(AcBz–N = CH–C_4H_9)⊂Co (3)

1 (153 mg, 0.5 mmol), valeraldehyde (pentanal) (129 mg, 1.5 mmol) and 20 mL of absolute ethanol were introduced in a 30 mL sealed microwave vessel. The mixture was placed under the microwave irradiation (30 W) for 10 min. The dark green powder was collected by filtration, washed with ethanol and dried under vacuum. Yield: 80%.

Anal. for $Co_2(OH)_{3.53}$(AcBz–N=CH–C_4H_9)$_{0.47}\cdot$2.9 H_2O: $Co_2C_{5.64}H_{10.11}N_{0.47}O_{4.47}\cdot$2.9 H_2O (M = 326.13 g mol^{-1}) found (%): Co, 36.17; C, 20.76; H, 3.23; N, 1.74; calcd: Co, 36.13; C, 20.77; H, 4.92; N, 2.02. IR (KBr pellet, cm^{-1}): 3426 (s), 2958 (m), 2930 (m), 2868 (w), 1603 (s), 1541 (s), 1387 (s), 1179 (m) 1056 (w), 786 (m).

(AcBz–N=CH–C_5H_{11})⊂Co (4)

1 (153 mg, 0.5 mmol), hexanal (150 mg, 1.5 mmol) and 20 mL of absolute ethanol were introduced in a 30 mL sealed microwave vessel. The mixture was placed under microwave irradiation (30 W) for 10 min. The dark green powder was collected by filtration, washed with ethanol and dried under vacuum. Yield: 80%.

Anal. for $Co_2(OH)_{3.57}$(AcBz–N=CH–C_5H_{11})$_{0.43}\cdot$2.3 H_2O: $Co_2C_{5.59}H_{10.45}N_{0.43}O_{4.43}\cdot$2.3 H_2O (M = 313.87 g mol^{-1}) found (%): Co, 37.29; C, 21.32; H, 3.83; N, 1.95; calcd: Co, 37.55; C, 21.39; H, 4.83; N, 1.92. IR (KBr pellet, cm^{-1}): 3425 (s), 2927 (m), 2858 (w), 1605 (s), 1539 (s), 1385 (s), 1179 (m), 789 (m), 618 (w), 507 (w).

(AcBz–N=CH–$C_{11}H_{23}$)⊂Co (5)

1 (153 mg, 0.5 mmol), dodecanal (276 mg, 1.5 mmol) and 20 mL of absolute ethanol were introduced in a 30 mL sealed microwave vessel. The mixture was placed under microwave irradiation (30 W) for 10 min. The dark green powder was collected by filtration, washed with ethanol and dried under vacuum. Yield: 80%.

Anal. for $Co_2(OH)_{3.49}$(AcBz–N=CH–$C_{11}H_{23}$)$_{0.51}\cdot$4.2 H_2O: $Co_2C_{9.69}H_{12.67}N_{0.51}O_{4.51}\cdot$4.2 H_2O (M = 407.12 g mol^{-1}) found (%): Co, 28.86; C, 28.35; H, 4.97; N, 1.86; calcd: Co, 28.95; C, 28.59; H, 6.48; N, 1.75. IR (KBr pellet, cm^{-1}): 3426 (s), 2925 (s), 2854 (s),

1603 (s), 1543 (s), 1386 (s), 1179 (m), 1098 (w), 1060 (w), 847 (w), 786 (m), 591 (w).

(AcBz–N=CH–Bz–CN)⊂Co (6is)

1 (153 mg, 0.5 mmol), 4-cyanobenzaldehyde (0.197 g, 1.5 mmol) and 20 mL of absolute ethanol were introduced in a 30 mL sealed microwave vessel. The mixture was placed under microwave irradiation (30 W) for 10 min. The dark green powder was collected by filtration, washed with ethanol and dried under vacuum. Yield: 80%.

Anal. for $Co_2(OH)_{3.51}(AcBz–N=CH–Bz–CN)_{0.49}\cdot 3.0\ H_2O$: $Co_2C_{7.35}H_{7.92}N_{0.98}O_{4.49}\cdot 4.2\ H_2O$ (M = 353.73 g mol^{-1}) found (%): Co, 33.26; C, 25.04; H, 3.02; N, 3.65; calcd: Co, 33.32; C, 24.96; H, 3.97; N, 3.88. IR (KBr pellet, cm^{-1}): 3432 (s), 2235 (m), 1593 (s), 1546 (s), 1385 (s), 1171 (m), 787 (w), 613 (w), 557 (w).

(AcBz–N=CH–Bz–CN)⊂Co (6ae)

LH (750 mg, 3 mmol) was dissolved in 50 mL of water and the pH was adjusted to 8 using 0.2 M NaOH. At this stage **$Co_2(OH)_3(OAc)\cdot H_2O$** (248 mg, 1 mmol) was added along with 20 mL of ethanol. The mixture was stirred under argon at room temperature for 48 h. The dark green powder was collected by filtration, washed with ethanol and dried under vacuum. Yield: 60%.

Anal. for $Co_2(OH)_{3.38}(AcBz–N=CH–Bz–CN)_{0.62}\cdot 1.0\ H_2O$: $Co_2C_{9.30}H_{8.96}N_{1.24}O_{4.62}\cdot 1.0\ H_2O$ (M = 347.89 g mol^{-1}) found (%): Co, 33.77; C, 32.28; H, 3.24; N, 4.68; calcd: Co, 33.88; C, 32.11; H, 3.18; N, 4.99. IR (KBr pellet, cm^{-1}): 3430 (s), 2235 (m), 1594 (s), 1543 (s), 1391 (s), 1170 (m), 1100 (w), 787 (w), 605 (w), 557 (m).

Acknowledgements

The authors thank the CNRS, the Université de Strasbourg and the Agence Nationale de la Recherche (ANR contract no. 2010-BLAN-913-01 (C-BLUE)). The European COST action MP1202 (HINT) is also gratefully acknowledged. The International Centre for Frontier Research in Chemistry (icFRC) is acknowledged for a post-doc grant. The authors thank A. Derory, C. Leuvrey and D. Burger for technical assistance, Dr J. Fouchet and Pr L. Douce for their help with the microwave oven.

Notes and references

1 A. K. Geim, *Science*, 2009, **324**, 1530–1534.
2 R. Ma and T. Sasaki, *Adv. Mater.*, 2010, **22**, 5082–5104.
3 P. Sun, R. Ma, M. Osada, T. Sasaki, J. Wei, K. Wang, D. Wu, Y. Cheng and H. Zhu, *Carbon*, 2012, **50**, 4518–4523.
4 J. N. Coleman, M. Lotya, A. O'Neill, S. D. Bergin, P. J. King, U. Khan, K. Young, A. Gaucher, S. De, R. J. Smith, I. V. Shvets, S. K. Arora, G. Stanton, H.-Y. Kim, K. Lee, G. T. Kim, G. S. Duesberg, T. Hallam, J. J. Boland, J. J. Wang, J. F. Donegan, J. C. Grunlan, G. Moriarty, A. Shmeliov, R. J. Nicholls, J. M. Perkins, E. M. Grieveson, K. Theuwissen, D. W. McComb, P. D. Nellist and V. Nicolosi, *Science*, 2011, **331**, 568–571.
5 M. Nagarathinam, K. Saravanan, E. J. H. Phua, M. V. Reddy, B. V. R. Chowdari and J. J. Vittal, *Angew. Chem., Int. Ed.*, 2012, **51**, 5866–5870.
6 *Functional Hybrid Materials*, ed. P. Gómez-Romero and C. Sanchez, Wiley-VCH, Weinheim, 2004.
7 Chem. Soc. Rev., 2011, 40, Themed issue on Hybrid Materials.
8 J. Mater. Chem., 2005, 15, Themed issue on Functional hybrid materials.
9 M. Li and S. Mann, *Angew. Chem., Int. Ed.*, 2008, **47**, 9476–9479.
10 C. Train, R. Gheorghe, V. Krstic, L.-M. Chamoreau, N. S. Ovanesyan, G. L. J. A. Rikken, M. Gruselle and M. Verdaguer, *Nat. Mater.*, 2008, **7**, 729–734.
11 A. Demessence, G. Rogez and P. Rabu, *Chem. Mater.*, 2006, **18**, 3005–3015.
12 A. Demessence, A. Yassar, G. Rogez, L. Miozzo, S. De Brion and P. Rabu, *J. Mater. Chem.*, 2010, **20**, 9401–9414.
13 E. Delahaye, S. Eyele-Mezui, J.-F. Bardeau, C. Leuvrey, L. Mager, P. Rabu and G. Rogez, *J. Mater. Chem.*, 2009, **19**, 6106–6115.
14 H. Shimizu, M. Okubo, A. Nakamoto, M. Enomoto and N. Kojima, *Inorg. Chem.*, 2006, **45**, 10240–10247.
15 E. Delahaye, S. Eyele-Mezui, M. Diop, C. Leuvrey, P. Rabu and G. Rogez, *Dalton Trans.*, 2010, **39**, 10577–10580.
16 E. Delahaye, S. Eyele-Mezui, M. Diop, C. Leuvrey, D. Foix, D. Gonbeau, P. Rabu and G. Rogez, *Eur. J. Inorg. Chem.*, 2012, 2731–2740.
17 S. Eyele-Mezui, E. Delahaye, G. Rogez and P. Rabu, *Eur. J. Inorg. Chem.*, 2012, 5225–5238.
18 G. Rogez, C. Massobrio, P. Rabu and M. Drillon, *Chem. Soc. Rev.*, 2011, **40**, 1031–1058.
19 R. Bourzami, S. Eyele-Mezui, E. Delahaye, M. Drillon, P. Rabu, N. Parizel, S. Choua, P. Turek and G. Rogez, submitted.
20 B. F. Hoskins and R. Robson, *J. Am. Chem. Soc.*, 1990, **112**, 1546–1554.
21 S. S.-Y. Chui, S. M.-F. Lo, J. P. H. Charmant, A. G. Orpen and I. D. Williams, *Science*, 1999, **283**, 1148–1150.
22 Z. Wang and S. M. Cohen, *Chem. Soc. Rev.*, 2009, **38**, 1315–1329.
23 S. M. Cohen, *Chem. Sci.*, 2010, **1**, 32–36.
24 K. K. Tanabe and S. M. Cohen, *Chem. Soc. Rev.*, 2011, **40**, 498–519.
25 S. M. Cohen, *Chem. Rev.*, 2012, **112**, 970–1000.
26 R. M. Abdelhameed, L. D. Carlos, A. M. S. Silva and J. Rocha, *Chem. Commun.*, 2013, **49**, 5019–5021.
27 K. Sumida and J. Arnold, *J. Chem. Educ.*, 2010, **88**, 92–94.
28 D. Bruhwiler, *Nanoscale*, 2010, **2**, 887–892.
29 A. Mehdi, C. Reye and R. Corriu, *Chem. Soc. Rev.*, 2011, **40**, 563–574.
30 E. Coronado, C. Marti-Gastaldo, E. N. Navarro-Moratalla and A. Ribera, *Inorg. Chem.*, 2010, **49**, 1313–1315.
31 G. Layrac, D. Tichit, J. Larionova, Y. Guari and C. Guerin, *J. Phys. Chem. C*, 2011, **115**, 3263–3271.
32 W. Ding, Z. Wei, S. Chen, X. Qi, T. Yang, J. Hu, D. Wang, L.-J. Wan, S. F. Alvi and L. Li, *Angew. Chem., Int. Ed.*, 2013, **52**, 11755–11759.

33 V. Laget, C. Hornick, P. Rabu and M. Drillon, *J. Mater. Chem.*, 1999, **9**, 169–174.
34 M. Louër, D. Louër and D. Grandjean, *Acta Crystallogr., Sect. B: Struct. Crystallogr. Cryst. Chem.*, 1973, **29**, 1696–1703.
35 L. Poul, N. Jouini and F. Fievet, *Chem. Mater.*, 2000, **12**, 3123–3132.
36 R. Ma, Z. Liu, K. Takada, K. Fukuda, Y. Ebina, Y. Bando and T. Sasaki, *Inorg. Chem.*, 2006, **45**, 3964–3969.
37 C. O. Kappe, *Chem. Soc. Rev.*, 2008, **37**, 1127–1139.
38 M.-H. Zeng, Y.-L. Zhou, W.-X. Zhang, M. Du and H.-L. Sun, *Cryst. Growth Des.*, 2009, **10**, 20–24.
39 A. Pons-Balague, N. Ioanidis, W. Wernsdorfer, A. Yamaguchi and E. C. Sanudo, *Dalton Trans.*, 2011, **40**, 11765–11769.
40 S. H. Jhung, J. H. Lee and J.-S. Chang, *Microporous Mesoporous Mater.*, 2008, **112**, 178–186.
41 K. J. Rao, B. Vaidhyanathan, M. Ganguli and P. A. Ramakrishnan, *Chem. Mater.*, 1999, **11**, 882–895.
42 A. N. Ergün, Z. Ö. Kocabaş, M. Baysal, A. Yürüm and Y. Yürüm, *Chem. Eng. Commun.*, 2013, **200**, 1057–1070.
43 D. Toulemon, B. P. Pichon, C. Leuvrey, S. Zafeiratos, V. Papaefthimiou, X. Cattoën and S. Bégin-Colin, *Chem. Mater.*, 2013, **25**, 2849–2854.
44 Y. Yoo, V. Varela-Guerrero and H.-K. Jeong, *Langmuir*, 2011, **27**, 2652–2657.
45 K. M. L. Taylor-Pashow, J. D. Rocca, Z. Xie, S. Tran and W. Lin, *J. Am. Chem. Soc.*, 2009, **131**, 14261–14263.
46 M. Kim, S. J. Garibay and S. M. Cohen, *Inorg. Chem.*, 2011, **50**, 729–731.
47 D. J. Lun, G. I. N. Waterhouse and S. G. Telfer, *J. Am. Chem. Soc.*, 2011, **133**, 5806–5809.
48 The size of the molecules was estimated using ChemBio3D (CambridgeSoft).
49 M. Nara, H. Torii and M. Tasumi, *J. Phys. Chem.*, 1996, **100**, 19812–19817.
50 V. Robert and G. Lemercier, *J. Am. Chem. Soc.*, 2006, **128**, 1183–1187.
51 G. B. Deacon and R. J. Phillips, *Coord. Chem. Rev.*, 1980, **33**, 227–250.
52 C. Dendrinou-Samara, G. Tsotsou, L. V. Ekateriniadou, A. H. Kortsaris, C. P. Raptopoulou, A. Terzis, D. A. Kyriakidis and D. P. Kessissoglou, *J. Inorg. Biochem.*, 1998, **71**, 171–179.
53 R. L. Carlin, *Magnetochemistry*, Springer-Verlag, Berlin, 1986.
54 E. M. Bauer, C. Bellitto, G. Righini, M. Colapietro, G. Portalone, M. Drillon and P. Rabu, *Inorg. Chem.*, 2008, **47**, 10945–10952.
55 P. Rabu, M. Drillon, K. Awaga, W. Fujita and T. Sekine, in *Magnetism: Molecules to Materials II. Molecules-Based Materials*, ed. J. S. Miller and M. Drillon, Wiley-VCH, Weinheim, 2001, pp. 357–395.
56 W. Fujita, K. Awaga and T. Yokoyama, *Inorg. Chem.*, 1997, **36**, 196–199.
57 M. Drillon and P. Panissod, *J. Magn. Magn. Mater.*, 1998, **188**, 93–99.
58 V. Laget, C. Hornick, P. Rabu, M. Drillon and R. Ziessel, *Coord. Chem. Rev.*, 1998, **178–180**, 1533–1553.
59 V. Laget, PhD thesis, Université Louis Pasteur, Strasbourg, France, 1998.